Environmental Science and Pollution Research
https://doi.org/10.1007/s11356-024-35195-5

RESEARCH ARTICLE

Lysosomal disruption, mitochondrial impairment, histopathological and oxidative stress in rat's nervous system after exposure to a neonicotinoid (imidacloprid)

Sarra Zouaoui[1,2] · **Rachid Rouabhi**[1,2]

Received: 30 August 2024 / Accepted: 26 September 2024

Abstract

Imidacloprid (IMI), a neonicotinoid pesticide, has been widely used due to its high efficiency against insect pests. However, its prolonged exposure may pose significant risks to non-target organisms, including mammals. Recent studies have raised concerns about its potential neurotoxicity, yet the underlying mechanisms remain poorly understood. This study aimed to assess the neurotoxic effects of chronic Imidacloprid exposure in *Wistar* rats, focusing on oxidative stress, mitochondrial dysfunction, and lysosomal disruption. *Wistar* rats were orally administered two doses of Imidacloprid (5 mg/kg and 50 mg/kg body weight) for three months. Neurotoxic effects were assessed by measuring key biochemical markers such as the enzymatic activities of catalase (CAT), glutathione peroxidase (GPx), superoxide dismutase (SOD), and glutathione S-transferase (GST). Non-enzymatic markers, including glutathione (GSH) levels and malondialdehyde (MDA) index, were also evaluated. Mitochondrial function was assessed by analyzing oxygen consumption, swelling, and membrane permeability and histopathological changes. Lysosomal stability was examined using the Neutral Red Retention Time (NRRT) assay. Neutral red is a dye that accumulates in the acidic environment of lysosomes. Healthy lysosomes retain the dye, while compromised lysosomes lose it, indicating destabilization. By measuring the amount of neutral red retained in lysosomes, the NRRT assay assesses lysosomal integrity. Lysosomal pH variations were also monitored to evaluate functional changes. Microscopic analysis provided insight into structural changes in lysosomes and other cell components. Lysosomal destabilization was further confirmed by morphological alterations observed through light microscopy, revealing a progressive, time-dependent

Responsible Editor: Lotfi Aleya

Highlights

- **Imidacloprid exposure** causes oxidative stress, mitochondrial impairment, and lysosomal destabilization in *Wistar* rats' central nervous system.
- **Decreased antioxidant enzyme activity** (CAT, GPx, and SOD) was observed, along with increased GST activity and elevated MDA levels.
- **Mitochondrial dysfunction** was evident, with alterations in oxygen consumption, swelling, and membrane permeability.
- **Lysosomal destabilization** was confirmed by Neutral Red Retention Time assay and Histological Tests further supported by structural alterations observed under microscopy.
- **Lysosomal pH elevation** indicated significant disruption in lysosomal function following Imidacloprid exposure.
- Clinical signs of intoxication-included lethargy, decreased activity levels, impaired motor coordination, and behavioral changes such as reduced exploratory behavior and altered grooming patterns.
- The study highlights the **neurotoxic potential** of chronic Imidacloprid exposure and its impact on cellular functions in the nervous system.

Extended author information available on the last page of the article

Published online: 02 October 2024

degeneration of lysosomal structures, including lysosomal expansion, neutral red dye leakage, and cell rounding. These changes reflected a temporal evolution of lysosomal damage, progressing from minor structural disruptions to more severe alterations as exposure continued, observable at the microscopic level. During the study, clinical observations of intoxicated rats included symptoms such as lethargy, reduced activity levels, and impaired motor coordination. High-dose Imidacloprid exposure led to noticeable behavioral changes, including decreased exploratory behavior and altered grooming patterns. Additionally, signs of neurotoxic effects, such as tremors or ataxia, were observed in the rats exposed to the higher dose, reflecting the systemic impact of chronic pesticide exposure. The results revealed a significant decrease in the enzymatic activities of CAT, GPx, and SOD, accompanied by an increase in GST activity. A notable reduction in glutathione levels and a rise in MDA index were observed, indicating enhanced oxidative stress in the brain. Mitochondrial impairment was evidenced by disturbances in oxygen consumption, increased swelling, and altered membrane permeability. Lysosomal destabilization was confirmed by reduced retention of neutral red dye, structural changes in lysosomes, and a significant rise in lysosomal pH in the IMI-exposed groups. In addition, the histopathological features indicate that imidacloprid at the given dose and exposure duration may have caused notable neurotoxic effects in *Wistar* rat brain tissue. Chronic exposure to Imidacloprid induces oxidative stress, mitochondrial dysfunction, lysosomal disruption and histopathological alterations in the central nervous system of *Wistar* rats. These findings provide valuable insights into the neurotoxic mechanisms of neonicotinoid pesticides, highlighting the need for further research to understand the long-term effects of Imidacloprid exposure on mammalian health.

Keywords Imidacloprid · Lysosomal destabilization · Neurotoxic · Mitochondria · Redox status markers · Microscopic study · Algeria

Introduction

The Industrial Revolution, coupled with rapid technological progress, has greatly intensified the release of hazardous substances in recent decades. This escalation has created a complex interplay between environmental degradation and public health, exacerbating the challenges faced in managing both issues (Andra et al. 2017; Andjelkovic et al. 2019).

To effectively evaluate risks, it is crucial to deeply understand the biochemical interactions of pesticides and their environmental impacts, which forms the foundation for precise risk assessment (Sakthiselvi et al. 2020; Zhao et al. 2020). As awareness grows regarding the potential impacts of pesticide use on ecosystems and human health, it is evident that their application comes with significant environmental and health risks, including acute and chronic poisoning (Fang et al. 2019; Bishop et al. 2020; Utami et al. 2020).

Neonicotinoids, a prominent class of pesticides, are particularly concerning due to their widespread use and potential for inducing oxidative stress in both humans and animals (Asghari et al. 2017; Wang et al. 2017). These pesticides, which include Imidacloprid, are used extensively in agriculture and on domestic pets, as well as for soil treatment and crop protection (Douglas and Tooker 2015; Cimino et al. 2017). Since their introduction in the late 1980s, neonicotinoids have been recognized for their efficacy but also for their potential to disrupt nervous system development and function (Simon-Delso et al. 2015; Julvez et al. 2016).

Neurotoxic effects from neonicotinoids can manifest through various behavioral, biochemical, physiological, and pathological changes in both the central and peripheral nervous systems. Imidacloprid, a widely used neonicotinoid, has been a key focus of studies due to its significant role in modern pest management and its potential to disrupt environmental and human health (Jeschke et al. 2011; Karahan et al. 2015). However, excessive use of these pesticides can lead to severe environmental imbalances and health hazards (Wang et al. 2018).

Mitochondria and lysosomes are crucial cellular organelles with significant roles in maintaining cell function and integrity. Disruptions in their functionality have been linked to various neurological disorders (Fraldi et al. 2016; Fivenson et al. 2017). Mitochondria, essential for energy production and calcium signaling, are particularly sensitive to damage, which can lead to a cascade of cellular dysfunctions and diseases (Pryde and Hirst 2011; Sun et al. 2016). Recent research suggests that mitochondrial impairment may be a primary target of neonicotinoid toxicity, with alterations in mitochondrial calcium homeostasis and respiration contributing to oxidative stress and cell death (Miao et al. 2022; Xu et al. 2022; Cestonaro et al. 2023).

Lysosomes, involved in the enzymatic degradation of cellular substances, are also affected by environmental stressors. The stability of lysosomal membranes can be assessed using neutral red, a cationic dye that accumulates in lysosomes and indicates membrane integrity (Duve 1963; Cesen et al. 2012). Changes in neutral red retention

can reveal lysosomal damage and dysfunction in response to various chemicals and pollutants. (Lowe et al. 1992).

This study aims to investigate the neurotoxic effects of Imidacloprid exposure in *Wistar* rats by examining its impact on oxidative stress, mitochondrial function, and lysosomal stability. It explores the relationship between pesticide exposure and neurotoxicity through both biochemical and microscopic analyses. The research offers novel insights into the mechanisms of neurotoxicity induced by Imidacloprid, focusing on its effects on mitochondrial and lysosomal functions. By combining biochemical assessments with detailed microscopic observations, it enhances our understanding of how neonicotinoids disrupt cellular processes and affect neurological health. For comprehensive risk assessment, it is crucial to consider the standard permissible limits of neonicotinoids in environmental matrices, as established by organizations such as the EPA, WHO, and FAO, which are essential for evaluating the safety and regulatory compliance of pesticide use (Table 1).

Materials and methods

Experiment design

In order to carry out our research study, we employed a particular experimental animal model, specifically adult male "*Wistar* albino rats." These rats were procured from the Algeria Pasteur Institute (API), which is renowned for its contributions to scientific research. The rats selected for the study had an average weight ranging between 240 and 300 g and were of similar size within the study parameters. Subsequently, we divided the animals into two distinct groups: a control group and a treatment group. were housed in spacious cages. Thirty rats were used in the study, and they were divided into three groups of ten rats each. upon arrival and maintained under controlled conditions: a temperature of 24 ± 4 °C, relative humidity of $60 \pm 10\%$, and a 12-h light/dark cycle. They had unrestricted access to food and water and were kept under standard hygiene conditions. After a four-week adaptation period, the rats were divided according to the studies by Duzguner and Erdogan (2010) and Kara et al. (2015).

The treatment involved daily gastric gavage with prepared solutions for 90 days. The groups were:

1. **Control Group (CT):** Rats in this group received only distilled water (1ml) via gavage for the entire 90-day period.
2. **Group II (IMI D1 group):** Rats in this group received a daily aqueous solution of Imidacloprid at a dose of 5 mg/kg/day.
3. **Group III (IMI D2 group):** Rats in this group received a daily dose of 50 mg/kg/day of Imidacloprid.

The study was conducted at the Toxicology Laboratory, Faculty of Applied Biology, Tebessa University, Algeria, adhering to Institutional Animal Care and Use Committee (IACUC) policies (Accreditation number: D01N01UN130120150006/2019).

Chemical product

Imidacloprid, a systemic neonicotinoid insecticide from the chloronicotinyl nitroguanidine family, was used in this study (CAS No. 138261–41-3, molecular formula

Table 1 The standard permissible limits of neonicotinoids in various matrices

Matrix	Pesticide	Agency	Permissible limit	Unit	Reference
Soil	Imidacloprid	EPA	0.1—1.0	mg/kg	EPA, 2021. "Pesticide Limits in Soil." EPA Website
	Clothianidin	EPA	0.5—1.0	mg/kg	EPA, 2021. "Pesticide Limits in Soil." EPA Website
	Thiamethoxam	EPA	0.1—0.5	mg/kg	EPA, 2021. "Pesticide Limits in Soil." EPA Website
Water	Imidacloprid	EPA	0.05—0.1	µg/L	EPA, 2021. "Pesticide Limits in Water." EPA Website
	Clothianidin	EPA	0.05—0.1	µg/L	EPA, 2021. "Pesticide Limits in Water." EPA Website
	Thiamethoxam	EPA	0.05—0.1	µg/L	EPA, 2021. "Pesticide Limits in Water." EPA Website
Plants	Imidacloprid	FAO	0.05—0.1	mg/kg	FAO, 2020. "Pesticide Residue Limits in Plants." FAO Website
	Clothianidin	FAO	0.05—0.1	mg/kg	FAO, 2020. "Pesticide Residue Limits in Plants." FAO Website
	Thiamethoxam	FAO	0.05—0.1	mg/kg	FAO, 2020. "Pesticide Residue Limits in Plants." FAO Website
Fish	Imidacloprid	WHO	0.1	mg/kg	WHO, 2019. "Pesticide Residue Limits in Fish." WHO Website
	Clothianidin	WHO	0.1	mg/kg	WHO, 2019. "Pesticide Residue Limits in Fish." WHO Website
	Thiamethoxam	WHO	0.1	mg/kg	WHO, 2019. "Pesticide Residue Limits in Fish." WHO Website
Animal Tissues	Imidacloprid	FAO	0.05—0.1	mg/kg	FAO, 2020. "Pesticide Residue Limits in Animal Tissues." FAO Website
	Clothianidin	FAO	0.05—0.1	mg/kg	FAO, 2020. "Pesticide Residue Limits in Animal Tissues." FAO Website
	Thiamethoxam	FAO	0.05—0.1	mg/kg	FAO, 2020. "Pesticide Residue Limits in Animal Tissues." FAO Website

C9H10ClN5O2). The chemical was sourced from Sigma Aldrich, Germany (Tomlin 2006).

Dose selection

Two doses of Imidacloprid (5 mg/kg and 50 mg/kg body weight) were administered to the animals for 90 days, dissolved in distilled water. Dose selection was based on previous studies, including those by Kara et al. (2015) and Duzguner and Erdogan (2010), and were within the non-toxic range, calculated relative to the LD50 values (424–475 mg/kg) to ensure safe daily exposure.

Mitochondria isolation from tissue

Mitochondria were isolated at 4°C using the following procedure: Resuspend the cell pellet from 1–2 mL of washed cells in ice-cold RSB hypo buffer (10 mM NaCl, 1.5 mM $MgCl_2$, 10 mM Tris–HCl, pH 7.5). Transfer the suspension to a Dounce or Potter–Elvehjem homogenizer and allow the cells to swell. After swelling, disrupt the cells with a tight-fitting pestle and verify lysis. Add 2.5 × MS homogenization buffer (210 mM mannitol, 70 mM sucrose, 5 mM Tris–HCl, pH 7.5, 1 mM EDTA) to the homogenate and transfer to a centrifuge tube for differential centrifugation. Centrifuge at 1,300 g for 5 min to remove nuclei, unbroken cells, and large debris. Collect the supernatant and repeat the centrifugation if necessary. Finally, centrifuge the supernatant at 7,000–17,000 g for 15 min to pellet the mitochondria, then wash and resuspend them in an appropriate buffer. For long-term storage, keep the mitochondria at -80°C for up to one year. Refer to Clayton and Shadel (2014) for detailed buffer recipes and protocol information.

Assessment of redox status markers

After a 3-month exposure period, rats were euthanized by decapitation, and the brain was collected and rinsed with cold phosphate-buffered saline (PBS). The redox status of mitochondrial matrix fractions was assessed by measuring protein content using the method of Bradford (1976), with bovine serum albumin as the reference standard.

Glutathione S-transferase (GST) activity was measured using the method of Habig et al. (1974), with absorbance recorded at 340 nm every 30 s for 3 min. Glutathione peroxidase (GPx) activity was determined by the method of Flohe (1984), with absorbance read at 420 nm. Catalase (CAT) activity was assessed following Aebi (1984), by monitoring the decomposition rate of H_2O_2 with absorbance at 240 nm. Superoxide dismutase (SOD) activity was evaluated using the method of Beauchamp and Fridovich (1971), where 50 µL of the matrix fraction was mixed with 2 ml of a reactive medium containing sodium cyanide (10–2 M), NBT solution (1.76 × 10–4 M), EDTA (66 mmol), methionine (10–2 M), riboflavin (2 µmol), and adjusted to pH 7.8 and exposed to light for 30 min to induce riboflavin's photoreaction. The resulting blue formazan was measured at 560 nm. Reduced glutathione (GSH) concentration was determined according to Weckbercker and Cory (1988), with absorbance at 412 nm, and malondialdehyde (MDA) levels were measured by the method of Warso and Lands (1983), detecting a red-colored complex with peak absorbance at 530 nm. Enzymatic activities were quantified in international units per milligram of protein.

Assessment of swelling, permeability and mitochondrial respiration

The impact of imidacloprid (IMI) on mitochondrial permeability transition pore (MPTP) was assessed by evaluating mitochondrial membrane permeability in the brain. Mitochondria were isolated from fresh brain tissue at 4°C and analyzed for swelling using the method described by Li et al. (2014). Equal volumes of isolated mitochondria were placed in quartz cells, and absorbance was monitored at 540 nm. A decrease in absorbance indicated increased mitochondrial swelling and loss of MPTP integrity. Mitochondrial respiration levels were measured using an Oxygraph (Hansatech) following the methods of Rouabhi et al. (2015) and Henine et al. (2016).

Isolation of lysosomes from rat brain

Based on De Duve and Wattiaux's 1963 technique, lysosomes were isolated from rat brain tissue as follows: The brain was collected, rinsed with cold phosphate-buffered saline (PBS), and free of meninges and blood. The tissue was cut into small fragments and homogenized in a pre-chilled glass or Potter–Elvehjem homogenizer with 0.25 M sucrose and 10 mM HEPES (pH 7.4). The homogenate was centrifuged at 1,000 g for 10 min at 4°C to remove large debris and nuclei. The supernatant was transferred to a new tube and centrifuged at 10,000 g for 20 min at 4°C to pellet the lysosomes. The lysosome pellet was resuspended in an appropriate buffer for further use. Throughout the procedure, maintaining a low temperature (4°C or on ice) was critical to prevent enzymatic degradation and preserve lysosome integrity.

Assessment of brain lysosomal stability by determination of neutral red retention time (NRRT)

Neutral red dye retention assay

Neutral red (CI 50040; Toluylene red chloride) was sourced from Sigma for the assay. This method is widely used to assess cell viability and cytotoxicity, particularly

in biomedical and environmental studies (Borenfreund and Puerner 1984; Repetto and Sanz 1993). The assay evaluates lysosomal membrane integrity, as neutral red selectively accumulates in lysosomes; damage reduces dye uptake. Following exposure to toxins, cells were fixed with formaldehyde, and neutral red was extracted using an acetic acid/ethanol mixture. Absorption was quantified using spectrophotometry at 540 nm, based on the protocol of Lowe et al. (1995) and PNEU/RAMOGE (1999).

Neutral red solution preparation

Dissolve 20 mg of Neutral Red powder in 1 ml of dimethyl sulfoxide (DMSO) to prepare the stock solution. Store in a dark container at room temperature. For the working solution, dilute 5 µL of the stock solution in 995 µL of phosphate-buffered saline (PBS). Prepare PBS by dissolving 4.77 g HEPES, 25.48 g NaCl, 13.06 g MgSO4, 0.75 g KCl, and 1.4 g $CaCl_2$ in 1 L of distilled water, adjust pH to 7.36 with 1M NaOH, and store in the refrigerator. Use the working solution at room temperature and store any unused solution in the dark at 4°C.

Toxicity determined *In Vitro* by morphological alterations and neutral red absorption

Microscopic study

The microscopic study of toxicity using morphological alterations and neutral red absorption involves observing cells under a light microscope with phase-contrast optics at ×400 magnification to identify structural changes indicative of cellular damage. Key alterations include cell shrinkage, membrane blebbing, and loss of adherence, vacuolization, and lysosomal damage, such as swelling or rupture. The neutral red dye accumulates in healthy lysosomes, so diminished uptake reflects lysosomal membrane disruption and overall cellular toxicity. These morphological observations provide critical insights into the extent and mechanisms of toxicity in vitro.

Histological tests

The histological tests were conducted following the method described by Houlot (1984), which involves several essential steps. First, the tissue samples are fixed in formalin and then placed in special perforated cassettes that allow the circulation of the liquids necessary for preparation. Next, the samples undergo progressive dehydration through a series of ethanol baths of increasing concentrations (70%, 95%, and 100%) and are then cleared in xylene to render the tissues transparent.

Once dehydrated, the tissues are embedded in liquid paraffin at 60°C. This step enables the paraffin to penetrate and impregnate the tissues. The following step is embedding, where the impregnated tissues are enclosed in paraffin blocks that, once solidified, facilitate cutting. These blocks are then sectioned into thin slices of 4 to 7 microns using a microtome. The resulting sections are placed onto glass slides for staining.

The standard staining method involves hematoxylin to stain the nuclei blue/violet, followed by eosin, which stains the cytoplasm and extracellular structures pink. After staining, the sections are mounted with cover slips and examined under a microscope for detailed tissue structure analysis. The sections are also photographed using a camera connected to a binocular magnifier. Histopathological anomalies, such as lesions, inflammation, or necrosis, can thus be accurately visualized.

Qualitative assessment of lysosomal ph variations

Brain organ samples are prepared by isolating and slicing the organ into 100–200 µm thick sections, which are then placed in a PBS buffer solution (1 g PBS powder per 100 mL distilled water) to preserve viability. pH-indicating probes are introduced by adding a working solution to the brain sections and incubating for 30 min to 1 h. Following incubation, the samples are washed and homogenized to remove excess probe. The homogenized sample is optionally centrifuged at 1,000 to 5,000 × g, and the supernatant is transferred to a micro-plate or cuvette for spectrophotometric pH measurement. pH variations are then assessed to determine lysosomal pH levels, following methods detailed by Fujiwara et al. (2009) for qualitative and quantitative analysis.

Statistical analysis

Data are presented as mean ± standard deviation (SD). Statistical analysis was performed using Minitab® software version 18.1 and Microsoft Excel version 19.0. Significant differences between treatment effects were evaluated using one-way ANOVA, followed by Tukey's post-hoc test for multiple comparisons. A p-value < 0.05 was considered statistically significant. Additionally, Student's t-test was used to compare group differences, with significance thresholds defined as: $*0.05 \geq p \geq 0.01$ (significant), $**0.01 \geq p \geq 0.001$ (highly significant), and $***p < 0.001$ (very highly significant).

Results

Clinical signs of intoxication

The clinical signs of intoxication observed in rats exposed to chronic Imidacloprid are summarized in Table 2. Rats

in the control group showed no significant clinical signs, maintaining normal activity and behavior. In the low-dose group (IMI D1, 5 mg/kg), mild symptoms were observed, including occasional lethargy, slight reductions in activity, occasional alterations in grooming behavior, minimal weight loss, and mild fur ruffing. Tremors, gait abnormalities, and respiratory distress were not commonly observed in this group. In contrast, the high-dose group (IMI D2, 50 mg/kg) exhibited pronounced neurotoxic effects, such as marked lethargy, frequent tremors, significant weight loss, impaired motor coordination, and altered exploratory behavior. Additional symptoms included frequent gait abnormalities, pronounced fur ruffing, and occasional seizures. Despite these pronounced symptoms, no mortalities were recorded in any of the groups. The severity and nature of clinical signs in the high-dose group underscore the dose-dependent neurotoxic impact of chronic Imidacloprid exposure, aligning with the observed biochemical and functional impairments in the study.

Assessment of redox status markers in brain mitochondria

The results of assessing various markers of mitochondrial redox status in the brains of rats after chronic exposed to imidacloprid at doses of 5 mg/kg and 50 mg/kg body weight are presented in Table 3. Glutathione (mitGSH), a crucial antioxidant tripeptide in brain mitochondria, showed a very highly significant ($p \leq 0.0001$) reduction in IMI-treated group (5/50 mg/kg/day) compared to the normal group. Additionally, the Table 3 indicates a significant increase ($P \leq 0.01$) in the enzymatic activity of the matrix glutathione S -transferase (mitGST) at 5 mg/kg/day and a very highly significant increase ($p \leq 0.0001$) at 50 mg/kg/day following a chronic exposition of the rats to imidacloprid in comparison with the control group. Furthermore, the enzymatic activity of glutathione peroxidase (mitGPx), a key antioxidant enzyme regulating ROS levels in the mitochondrial matrix, has been decreased with very highly significant manner ($p \leq 0.0001$), (Table 3) in IMI-treated rats at the higher dose compared to control group. A very highly significant decrease ($p \leq 0.0001$) was also observed in brain mitochondrial catalase activity in the IMI-treated group at 50 mg/kg/day compared to the control. Moreover, the activity of superoxide dismutase enzyme (mitSOD) was highly significantly ($p \leq 0.01$) decreased at 5mg / kg / day and showed a very highly significant decrease ($p \leq 0.0001$) at 50 mg/kg/day after 90 days of imidacloprid exposure compared to the control group. Levels of Malondialdehyde (mitMDA) in brain mitochondria, indicating oxidative stress impact on lipid compounds, were very highly ($p \leq 0.0001$) significantly increased in brain mitochondria at 50 mg/kg/day and highly significantly increased ($p \leq 0.01$) at 5mg / kg / day in the IMI-treated rats compared to the control group (Table 3). These findings demonstrate that the severity of these changes is dose-dependent.

Study of mitochondrial apoptosis parameters

The toxicological effects of imidacloprid on mitochondrial integrity and function parameters (Including swelling, permeability, respiration) in the brains of *Wistar* rats is presented in Table 4. The study results indicate a very highly significant increase ($p \leq 0.0001$***) in mitochondrial

Table 2 Clinical signs and mortality in rats exposed to chronic imidacloprid

Clinical signs	Control group	IMI D1 Group (5 mg/kg)	IMI D2 Group (50 mg/kg)
Behavioral Changes	No significant clinical signs	Occasional alterations in grooming behavior	Decreased exploratory behavior, altered grooming patterns
Impaired Motor Coordination	Not observed	Not observed	Impaired motor coordination, ataxia
Decreased Activity	No significant clinical signs	Mild lethargy, slight reduction in activity	Pronounced lethargy, reduced activity levels
Tremors	Not observed	Occasional	Frequent
Loss of Appetite	Not observed	Mild	Moderate to Severe
Weight Loss	Not observed	Minimal	Significant
Gait Abnormalities	Not observed	Occasional	Frequent
Fur Ruffing	Not observed	Mild	Pronounced
Seizures	Absent	Absent	Occasional
Respiratory Distress	Not observed	Not observed	Mild
Diarrhea	Not observed	Not observed	Occasional
Overall Clinical Summary	No significant clinical signs	Milder signs, such as slight reductions in activity	Pronounced neurotoxic effects, consistent with biochemical and functional impairments
Percentages of Mortalities	0%	0%	0%

Table 3 Variation of mitochondrial oxidative stress parameters in rats' brain in control and treated rats after three months of treatment under the effect of imidacloprid chronic exposure at the dose of 5 and 50 mg/kg body weight

Antioxidant parameters	Experimental groups		
	Control group	Treated groups	
		IMI (5mg / kg / day)	IMI (50mg / kg / day)
Mit GSH µmol/mg	0.00049075 ± 8.9837E-06	0.00046 ± 1.73861E-05 ***	0.000391 ± 1.59844E-05 ***
Mit GPx µmol/min/mg	1.06901 ± 0.04135198	1.03118 ± 0.020193 **	1.0014 ± 0.06858139 ***
Mit GST µmol/min/mg	0.0051075 ± 0.000817068	0.007833 ± 0.000383 *	0.012335 ± 0.0006304 ***
Mit CAT µmol/min/mg	0.000422 ± 7.06122E-06	0.00031 ± 1.23107E-05 **	0.000251 ± 1.59814E-05 ***
Mit MDA nmol/mg	3.0001756 ± 0.18572284	4.60657 ± 0.20035576 **	5.001675 ± 0.00610983 ***
Mit SOD U/mg	17.13205 ± 0.135972041	15.008 ± 0.617202 **	13.1428 ± 0.53696281 ***

Each value is presented as the mean ± standard deviation, and the Student's t-test was employed for analysis. Batch comparison between the treated and control groups was conducted. Significance levels were defined as follows: ($P \leq 0.05$): significant (*), ($p \leq 0.01$): highly significant (**), ($p \leq 0.0001$): very highly significant (***), $P > 0.05$: not significant (ns)

swelling at a dose of 50 mg/kg/day of IMI (Table 4; Fig. 1), which is directly proportional to the absorbance values. Additionally, there was a significant increase ($p \leq 0.05$*) in mitochondrial swelling when rats were exposed to 5 mg/kg/day of IMI for an extended period compared to the control group (Fig. 2). On the other hand, the assessment of mitochondrial permeability measured as the change of mitochondrial size over time, following the addition of calcium to mitochondrial suspension (Table 4; Fig. 3). In addition, the results of this essay are represented by a kinetic curve (Table 4) which demonstrated a significant difference between IMI-treated group and normal group with significance degree of p. Furthermore, the evaluation of respiratory function of brain mitochondria revealed a highlighted a significant decrease in oxygen consumption rate in IMI-treated rats compared to non-IMI-exposed animals (Table 4; Fig. 2).

Assessment of brain lysosomal stability by determination of neutral red retention time (NRRT)

The effect of imidacloprid exposure on the rate of incorporation of the RN by the viable cells after 24, 48 h indicates significant differences ($P \leq 0.05$) at the specified concentrations compared to the control at both time points. Experiments (n = 6) were performed in triplicate, and the data are presented as mean ± standard error (SE) in Table 5; Fig. 4.

- **Control group:** In this group, absorbance at 540 nm is measured for brain cells without treatment. The initial absorbance gives a reference to compare with the other groups.
- **Group treated with 5 mg/kg of IMI (Imidacloprid):** After 24 h, we observed an increase in absorbance com-

Table 4 Brain swelling, respiration, and mitochondrial permeability in control and treated rats following three months of treatment

Mitochondrial apoptosis parameters	Experimental groups		
	Control group	Treated imidacloprid groups	
		IMI (5mg / kg / day)	IMI (50mg / kg / day)
Mitochondrial Swelling as (optic density)	0,1966 ± 0,00947629	0,219 ± 0,03117691 *	0,3426 ± 0,01393915 ***
Mitochondrial Respiration as O_2 Consumption	+ + + + +	+-	+ + +
Mitochondrial Permeability as (ΔOD/Δt)	0,0325943 ± 0,0026469 + + +	0,0339086 ± 0,0010595 + + +	0,063383 ± 0,0011607 *** + + + + +

Mean ± SE.t-test was used for multiple comparisons. ($P \leq 0.05$): significant (*), ($p \leq 0.01$): highly significant (**), ($p \leq 0.0001$): very highly significant (***), $P > 0.05$: not significant (ns)

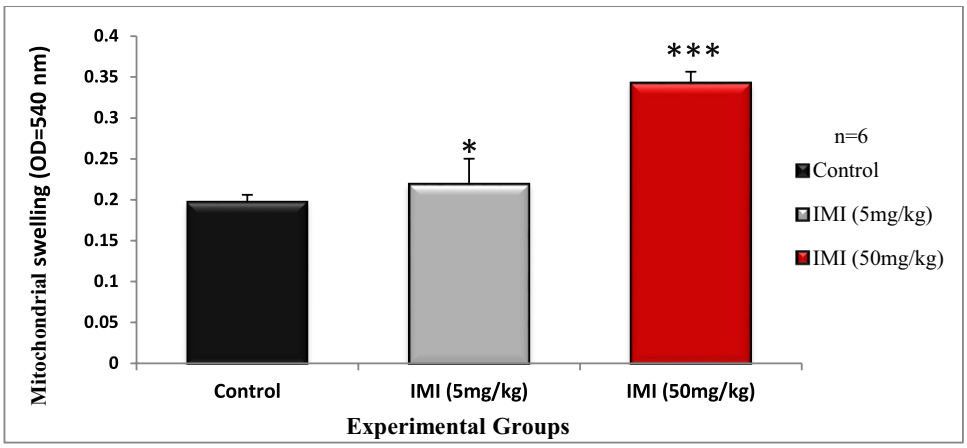

Fig. 1 Effect of IMI on mitochondrial swelling at OD540 nm after 90 days. Each value is expressed as mean ± standard deviation, we use Student test. Batch Compare treated with Imidacloprid (IMI) and control group. ($P \leq 0.05$): significant (*), ($p \leq 0.0001$): very highly significant (***), $P > 0.05$: not significant (ns)

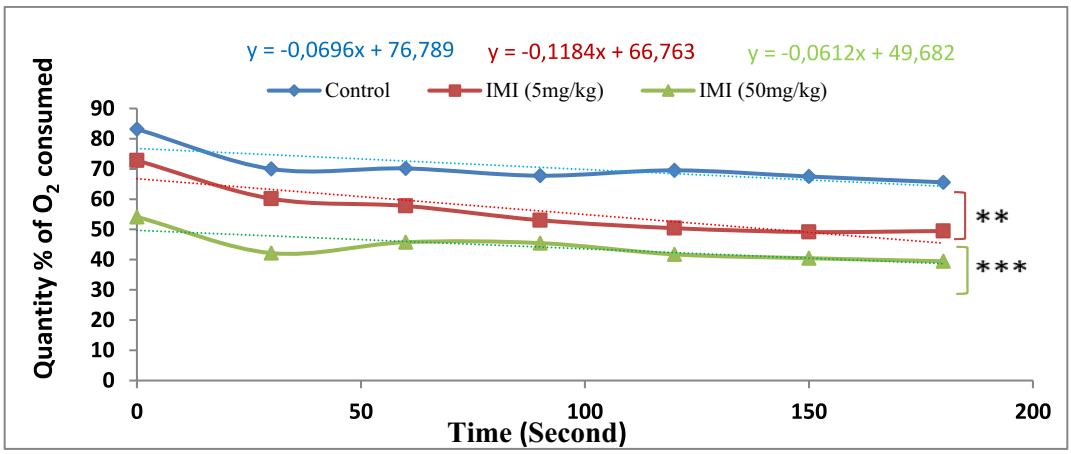

Fig. 2 Effect of oral administration of IMI at different doses on mitochondrial respiration (nmol/ml) after 90 days. $n = 6$ rats/group. Results in each group represent mean ± SEM; ($p \leq 0.01$): (**), ($p \leq 0.0001$): (***)

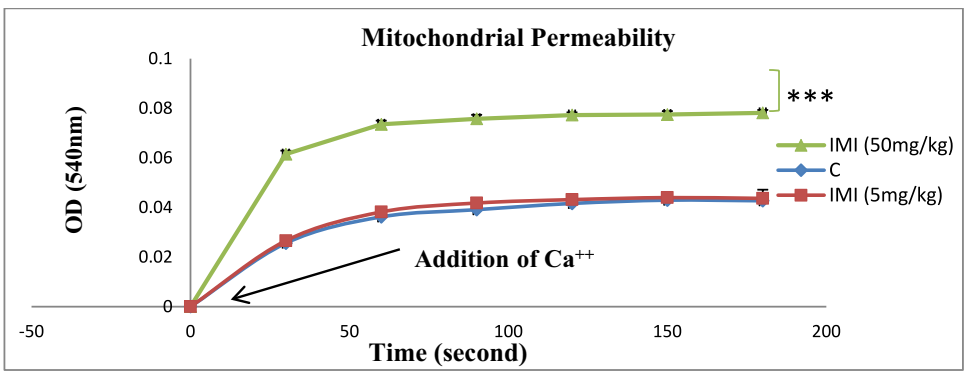

Fig. 3 Effect of IMI on mitochondrial permeability after 90 days. Results in each group represent mean ± SEM., ($p \leq 0.0001$): (***), ($n = 6$ rats/group)

pared to the control group. This could indicate that brain cells have absorbed the neutral red or undergone changes in lysosomes. After 48 h, absorbance could decrease as lysosomes destabilize, releasing neutral red into the cytosol and resulting in cell death.

- **Group treated with 50 mg/kg of IMI:** After 24 h, we see a more pronounced increase in absorbance compared to the control group due to the higher dose of IMI. After 48 h, a more significant decrease in absorbance occurs, indicating faster lysosome destabilization and more pronounced cell death. In summary, after 24 h, absorbance increase in the treated groups due to the absorption of neutral red by lysosomes. After 48 h, absorbance decrease due to lysosome destabilization

Table 5 Assessment of imidacloprid's effects on absorbance at 540 nm: Comparative analysis across variable groups and doses over time

Variable groups		Control	IM (5mg / kg / day)	IM (50mg / kg / day)
Absorbance at 540 nm	For (A) 24 h	3,595 ± 0,26,154,197	3,795 ± 0,24,146,697 *	4,264 ± 0,42,916,349 *
	For (B) 48 h	4,1 ± 0,19,962,465	3,081 ± 0,21,739,641 *	2,806 ± 0,29,236,963 **

Results are expressed as mean ± SE.t-test was used for multiple comparisons. ****$P < 0.0001$, ***$P < 0.001$, **$P < 0.01$, *$P < 0.05$ statistical significant as compared to control. *IMI* Imidacloprid, ($n = 5$)

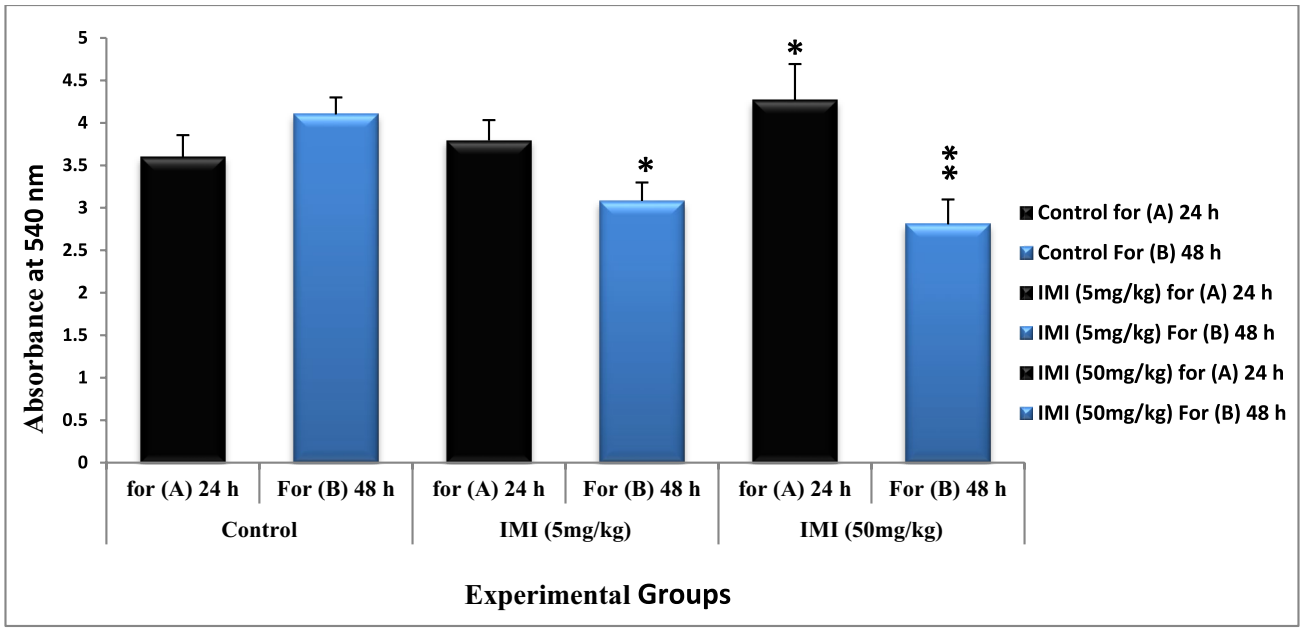

Fig. 4 Effect of Imidacloprid in different treatment groups, on the brain cells of retention of neutral red. indicate significant differences ($p < 0.05$; Tukey's test) between means ± SE. absorbance values (540 nm) measured with the neutral red assay to evaluate the lysosome destabilization of brain cells incubated for **A** 24 h and **B** 48 h ($n = 6$). Error bars present standard deviation

and the release of neutral red into the cytosol, leading to cell death.

Morphological alterations [microscopic observations (× 400)]

The results of Microscopic examination under a light microscope equipped with phase-contrast optics at a magnification of × 400 following exposure to imidacloprid after a neutral red assay, were presented in Fig. 5, 6, 7 and 8. Showed the morphological alterations following the designated exposure periods, cells are carefully observed with a specific focus on identifying indications of disruption in the structural integrity of the lysosomal membrane.

An NRR assay on *Wistar* rat brain cells exposed to Imidacloprid yielded intriguing findings: [1] Exposed cells exhibited "rounding-up," indicating a change in shape towards a more spherical form. [2] The rounding-up appeared linked to the leakage of neutral red dye into cell cytosol, suggesting a disruption in cellular membrane integrity due to Imidacloprid exposure. [3] The presence of granulocytes with small lysosomes was noted, hinting at potential impacts on these white blood cells, including alterations in lysosomal structures and functions as a consequence of imidacloprid exposure.

Over time, this sample underwent a dynamic temporal transformation characterized by a trilogy of events: [1] firstly, an expansion and augmentation of the lysosomal compartment; [2] secondly, the gradual seepage of NR dye into the cytoplasm; and ultimately, culminating in a cell-rounding phenomenon as the final evolutionary progression [3].

Undoubtedly, the lysomotropic dye, neutral red, exhibits a proclivity for lysosomal retention, a phenomenon characterized by a progressive escalation in lysosomal volume during the incubation period. This trend persists until it reaches a critical point where the lysosomal membrane experiences destabilization, subsequently leading to the efflux of neutral red into the cytosolic milieu.

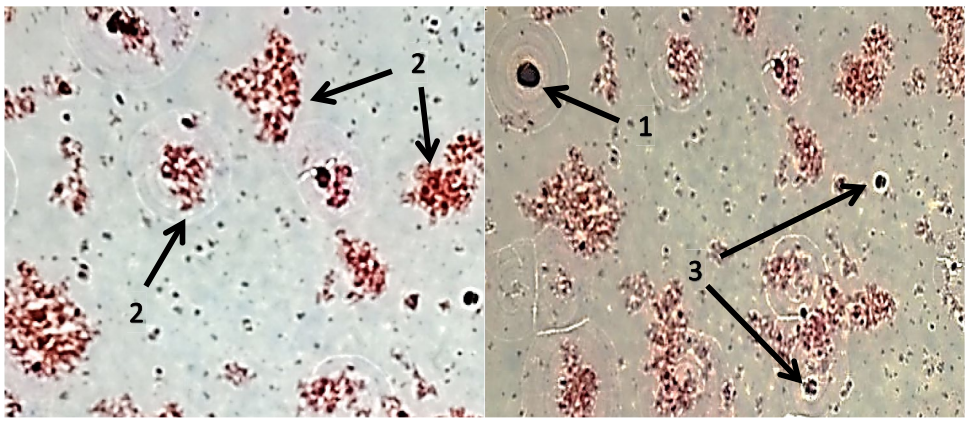

Fig. 5 Indications of a disturbance in the structural integrity of the lysosomal membrane

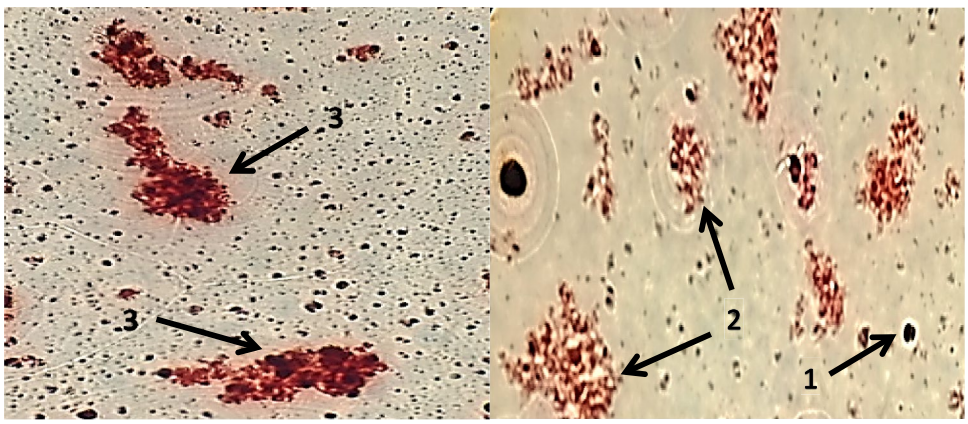

Fig. 6 Temporal metamorphosis: the trilogy of transformative events in sample evolution

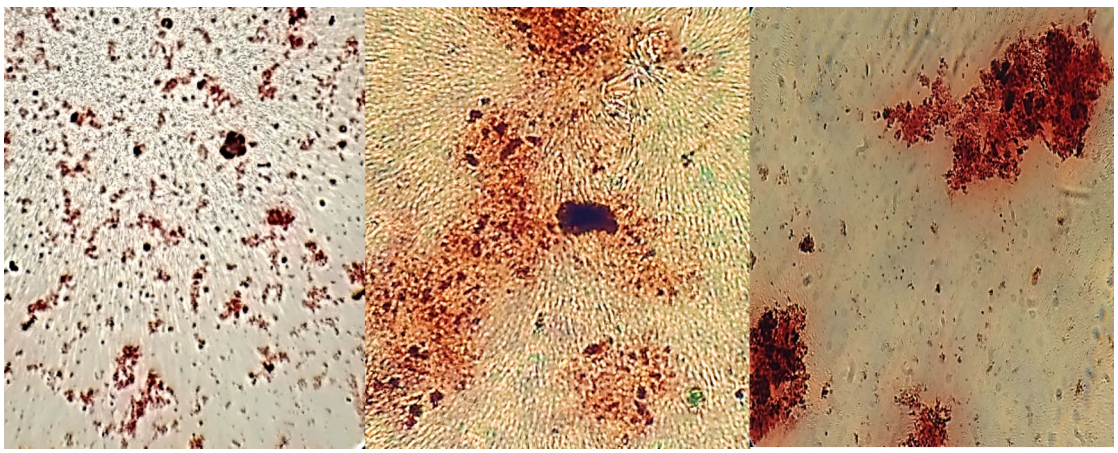

Fig. 7 Lysosomal dynamics**:** the retention and release of neutral red

The study examines the relationship between incubation time and absorbance at 540 nm after a neutral red assay, following exposure to Imidacloprid, at various time intervals (0h, 2h, 4h, 6h, and 8h).

The initial time point (0h), establishes a baseline measurement reflects the immediate impact of Imidacloprid exposure. At 2 h (2h), early cellular responses and adaptations are observed, potentially indicating changes in lysosomal volume and neutral red leakage. The 4-h (4h) mark represents a pivotal stage in the incubation period, reflecting significant cellular alterations. By 6 h (6h), late-stage responses or stabilization of observed effects becomes apparent. The final time point, 8 h (8h), offers insights into cumulative and late-stage responses and the saturation of cellular changes.

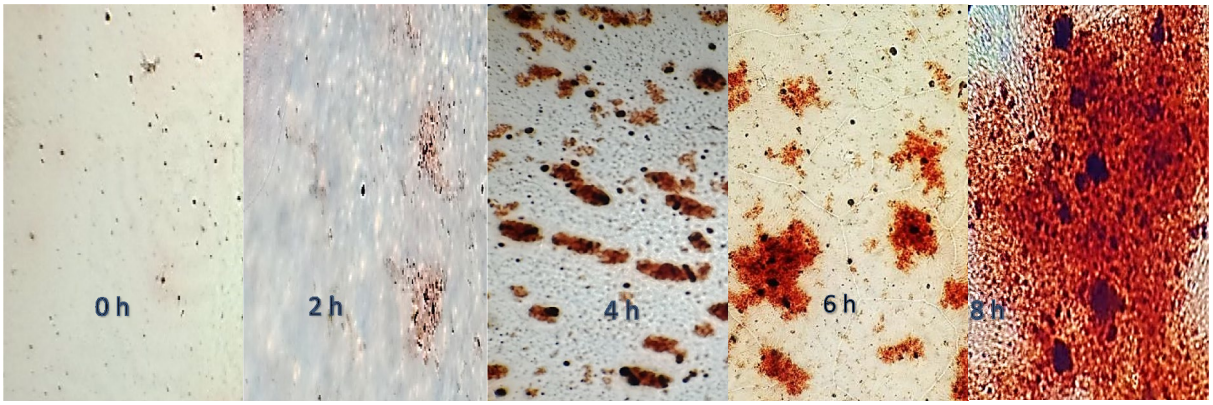

Fig. 8 The correlation between the time of incubation with neutral red and the subsequent absorbance at 540 nm following the neutral red assay

Histopathological examination

Figure 9 illustrates histopathological changes in the brains of *Wistar* rats after 90 days of Imidacloprid exposure. The control group shows normal neuronal architecture with no signs of degeneration or inflammation. In the low-dose group (5 mg/kg/day), there is marked disorganization of nerve fibers, vacuolization, neuronal loss, and mild glial cell infiltration, indicating neurotoxicity and an inflammatory response. The high-dose group (50 mg/kg/day) displays severe neurotoxic effects, including early cerebral necrosis, tissue degradation, and signs of mild tissue edema, suggesting progressive brain damage and disruptions in the blood–brain barrier.

Pathological and morphological changes observed in the brain and other tissues

The Table 6 highlights dose-dependent pathological changes in rats exposed to Imidacloprid. The control group showed no significant changes, while the low-dose group (5 mg/kg) exhibited mild neuronal degeneration and slight vacuolization. In contrast, the high-dose group (50 mg/kg) showed pronounced neuronal degeneration, severe vacuolization, lysosomal destabilization, and disrupted cellular architecture, indicating severe neurotoxic effects. leading to the highest total pathological score. The scores reflect the escalating severity of neurotoxic damage with increasing doses of Imidacloprid.

Qualitative assessment of lysosomal ph variations

Measuring the ph levels inside lysosomes

The results of assessments of lysosomal pH variations during chronic exposure on brain cells in control and IMI-treated rats were presented in Figs. 10 and 11 demonstrated a significant increase in lysosomal pH in brain cells among the IMI-exposed groups, with the magnitude of the increase varying with the IMI dose.

Discusion

The current study aimed to evaluate the neurotoxic impact of exposure to Imidacloprid (IMI) on *Wistar* rat brains (5 and 50mg/kg body weight; orally) for three months. Various parameters, including redox status markers (GST, GPX, GSH, MDA, SOD, CAT) Results were shown in Table 2, Clinical Signs and Mortality. Table 3, mitochondrial stress parameters (Table 4; Figs. 1, 2 and 3), lysosomal stability (Table 5, Fig. 4), cellular morphology (Figs. 5, 6, 7 and 8), histopathological changes (Fig. 9) and pH variations (Figs. 10 and 11), were analyzed, to understand the underlying neurotoxic mechanisms.

Clinical signs and mortality rates observed in our study (Table 3) provided additional insights into the neurotoxic potential of IMI. High-dose exposure (50 mg/kg) was associated with pronounced clinical symptoms, including ataxia, tremors, and lethargy, which reflect central nervous system impairment were consistent with previous reports of neurobehavioral alterations and toxicity associated with IMI exposure. Bomann (1989) and Pauluhn (1988) also documented clinical symptoms such as tremors and ataxia in pesticide-treated animals, similar to the symptoms observed in the current study. In our study, no mortality was observed in any of the treatment groups throughout the experimental period, indicating that the administered doses of Imidacloprid were not lethal to the rats. Conversely, in laboratory studies involving rats, the median lethal dose (LD50) for imidacloprid was found to be approximately 424 mg/kg for male rats and between 450–475 mg/kg for female rats. Mortality was first observed at doses of 400 mg/kg, with a rapid increase to 100% mortality at 500 mg/kg. (Sheets 2001).

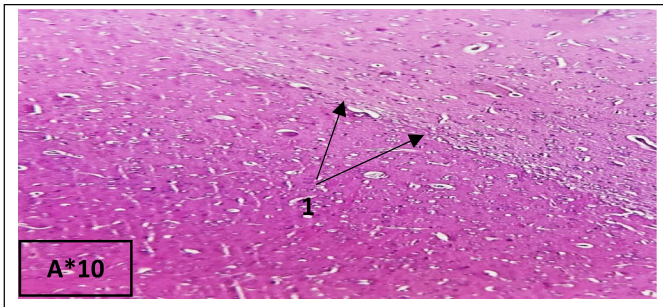

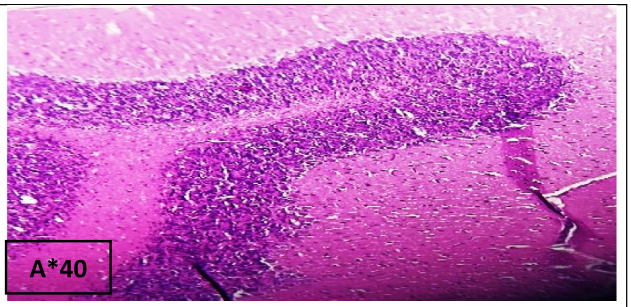

Histological section of the brain from a *Wistar* rat in the control group after 90 days of treatment, showing normal neuronal architecture with well-preserved neuronal cell bodies, no vacuolization, and absence of pathological alterations such as necrosis or inflammation. No significant neuronal degeneration is present, indicating tissue integrity. **Staining: Hematoxylin-Eosin (H&E), magnification x10/x40.**

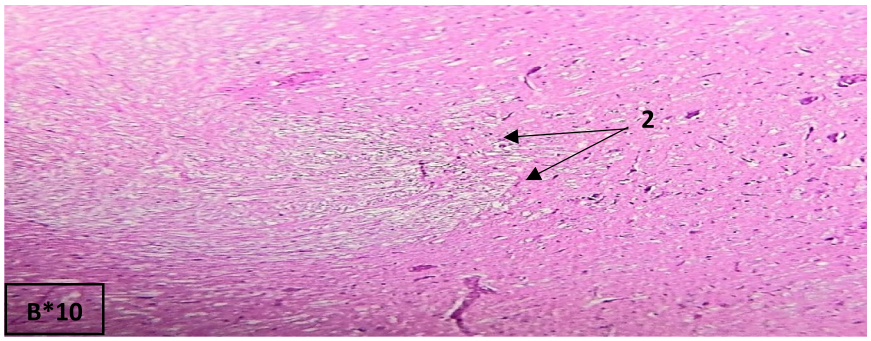

Histological section of the brain from a *Wistar* rat exposed to imidacloprid (5 mg/kg/day) for 90 days. Microscopic analysis shows signs of neurotoxicity, characterized by marked disorganization of nerve fibers and loss of normal brain tissue architecture. Areas of vacuolization and neuronal loss are observed, indicating damage to neuronal cells. The brain structure also shows evidence of mild glial cell infiltration, suggesting an inflammatory response to chronic pesticide exposure. **Stained with Hematoxylin-Eosin (H&E).Magnification x10.**

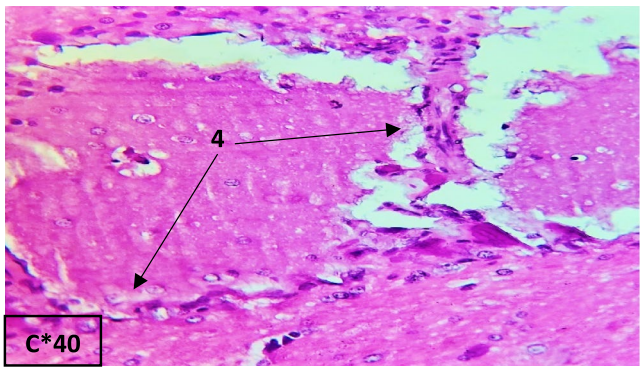

Histological section of the brain from a *Wistar* rat treated with imidacloprid (50 mg/kg/day) for 90 days. Microscopic analysis reveals the early stages of cerebral necrosis (D2), characterized by localized cell death and tissue degradation. These findings suggest significant neurotoxicity, with marked disruption in the brain's architecture and early necrotic changes. **Stained with Hematoxylin-Eosin (H&E). Magnification x40.**

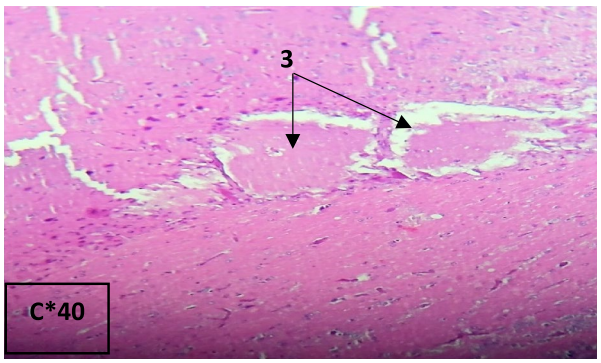

Histological section of the brain from a *Wistar* rat treated with imidacloprid (50 mg/kg/day) for 90 days. Microscopic analysis shows the presence of regular spaces (regular port spaces), indicating mild tissue edema or early neuro-inflammatory responses. These changes suggest potential disruptions in the blood-brain barrier or fluid accumulation within the brain. While neuronal structures remain visible, these pathological signs point to progressive brain damage due to prolonged exposure to imidacloprid. **Stained with Hematoxylin-Eosin (H&E). Magnification x40.**

Fig. 9 Histological Sections (×10/40) of the brain after oral administration of imidacloprid in control and treated rats following three months of treatment. **A** Control**, B** Treated with IMI 5 mg/kg/day, **C** Treated with IMI 50 mg/kg/day, (1): Glial Cells; (2): Nerve Fibers. (3): Regularly spaced portal areas. (4): Tissue degradation

Alterations in oxidative balance, such as increased levels of reactive species or reduced efficiency of radical scavenging systems, can compromise cellular integrity. Cellular antioxidant defenses consist of both non-enzymatic antioxidants like GSH and enzymatic antioxidants such as SOD, CAT, and GST, working together to alleviate oxidative stress (Mehta and Gowder 2015).

Table 6 Pathological and morphological changes observed in the brain and other tissues, along with the pathological scores for each dose group

Dose group	Pathological/Morphological changes observed	Neuronal degeneration	Vacuolization	Lysosomal destabilization	Glial Cell activation	Mitochondrial swelling	Total pathological score
Control Group	No significant pathological changes observed	0	0	0	0	0	0
IMI D1 Group (5 mg/kg)	Mild neuronal degeneration, slight vacuolization, minor lysosomal changes	1	1	1	0	0	3
IMI D2 Group (50 mg/kg)	Pronounced neuronal degeneration, extensive vacuolization, severe lysosomal destabilization, increased glial cell activation, mitochondrial swelling, and disruption of cellular architecture	3	3	3	2	2	13

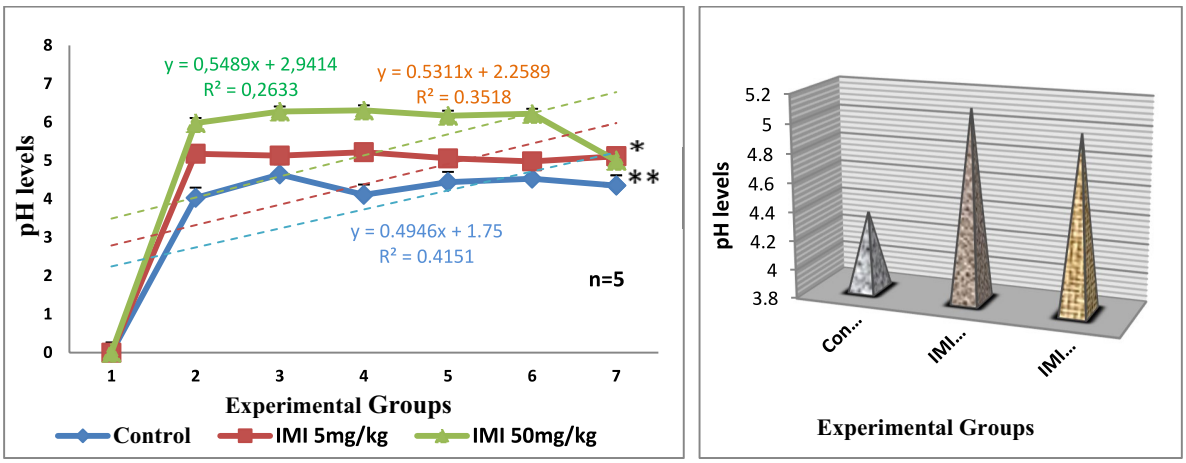

Fig. 10 The effect of Imidacloprid on lysosomal pH during chronic exposure on brain cells in control and treated rats. Results are expressed as mean ± SE.t-test was used for multiple comparisons, $^{**}P<0.01$, $^{*}P<0.05$ statistical significant as compared to control. IMI: Imidacloprid, ($n=5$)

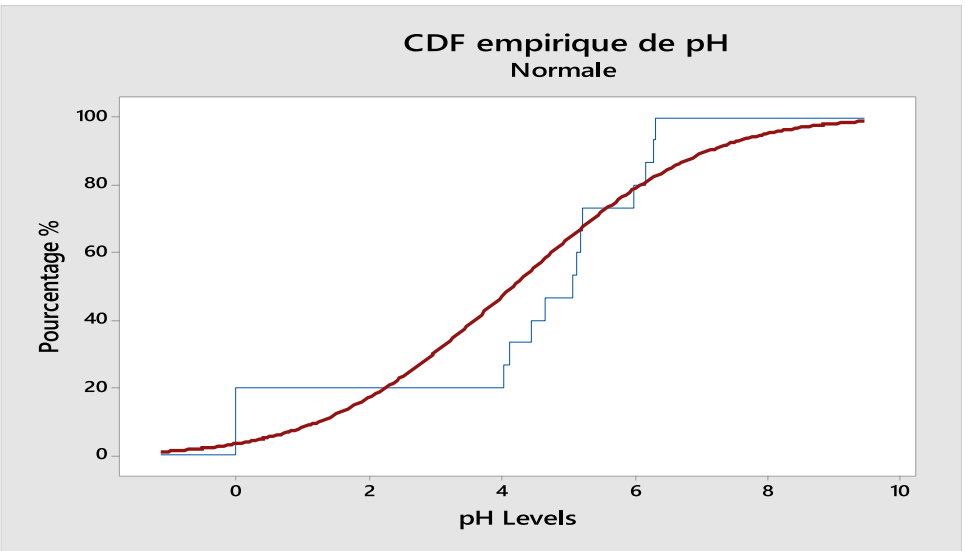

Fig. 11 Empirical CDF (cumulative distribution function) of pH represents the cumulative probability of pH values in different groups in the whole brain of rats treated for **3** months with IMI. ($n=15$). IMI: Imidacloprid

Our findings reveal a statistically significant increase in Malondialdehyde (MDA) levels in rats treated with Imidacloprid, showing a highly significant elevation ($p \leq 0.0001$) at a dose of 50 mg/kg/day and a significant increase ($p \leq 0.01$) at 5 mg/kg/day compared to the control group (Table 3). This indicates enhanced oxidative damage and lipid peroxidation. MDA serves as a biomarker for lipid oxidative damage, particularly from the peroxidation of polyunsaturated fatty acids (Zhang et al. 2004). The proposed mechanism suggests that free radicals generated by Imidacloprid exposure inhibit antioxidant enzymes, contributing to increased oxidative stress. These findings enhance our understanding of the potential adverse effects of Imidacloprid on oxidative stress in the brain.

Similarly, previous studies have reported altered oxidative stress and lipid peroxidation markers in rats exposed to Imidacloprid (Mohany et al. 2011; Balani et al. 2011). Additionally, Birsen (2011) demonstrated that exposure to thiacloprid, another neonicotinoid insecticide, at doses of 112.5 and 22.5 mg/kg/day for 30 days significantly elevated MDA levels in lymphoid organs. Ince et al. (2013) also reported that oral administration of Imidacloprid at 15 mg/kg/day for 28 days resulted in a significant increase in MDA levels, along with decreased SOD and catalase activities in mice.

According to our biochemical analysis, the enzymatic activity of glutathione S-transferase (GST) very highly significantly increased ($p \leq 0.0001$) in the Imidacloprid-treated group at the higher dose compared to the control group (Table 3). GST utilizes glutathione as a cofactor, and the observed reduction in GST levels in our study may be attributed to the consumption of glutathione as it acts to protect against Imidacloprid-induced toxicity (Danyelle and Kenneth 2003). These findings align with those of Lonare et al. (2014), who reported the activation of detoxification mechanisms in rats following oral administration of Imidacloprid at doses of 45 and 90 mg/kg, noting increased activity of detoxification enzymes, including glutathione (GSH) and GST, compared to controls.

Our results also reveal a significant decrease in the activities of glutathione peroxidase (GPx) and catalase (CAT) in treated rats compared to the control group (Table 3). This decline is likely due to the depletion of cellular antioxidant defenses against reactive oxygen species (ROS) generated by Imidacloprid exposure. Reduced GPx and CAT activity can lead to the accumulation of hydrogen peroxide (H_2O_2), which subsequently generates hydroxyl radicals (OH°) through the Fenton reaction (Cory-Slechta et al. 2005). Multiple independent studies support these observations (Mikolić and Karačonji 2018), consistent with findings from a meta-analysis by Coremen et al. (2022), which highlighted a strong link between pesticide exposure and changes in various biochemical markers in rats.

In this study, a significant decrease in mitochondrial GSH levels was observed in the treated rats compared to the control group (Table 3). GSH plays a crucial role in protecting the brain from oxidative stress, with its regulation and production limited by the transport of thiol amino acids across the blood–brain barrier (Valdovinos-Flores and Gosenbatt 2012). GSH exists in reduced (GSH) and oxidized (GSSG) forms, both of which are essential for neutralizing reactive oxygen species (ROS) (Daubié, 2011).

Our findings are consistent with previous research showing a reduction in mitochondrial GSH levels following 21 days of treatment with various doses of pyrethroids, attributed to excessive ROS generation (Ashar Waheed and Muthu Mohammed 2012; Dar et al. 2013; Mani et al. 2014).

Our findings indicate that rats treated with Imidacloprid (IMI) experienced a very highly significant decrease ($p \leq 0.0001$) in superoxide dismutase (SOD) levels at a dosage of 50 mg/kg/day, and highly significant reduction ($p \leq 0.01$) at 5 mg/kg/day (see Table 3). This reduction in SOD activity suggests that Imidacloprid plays a role in the conversion of superoxide (O^{-2}) to hydrogen peroxide (H_2O_2).

Our findings align with Kapoor et al. (2010) that conducted a study examining the effects of sub-chronic dermal exposure to Imidacloprid in female rats, which yielded similar findings related to SOD and catalase (CAT) activities and lipid peroxidation levels. In contrast, EL-Gendy et al. (2010) reported that administering 15 mg/kg of Imidacloprid resulted in significant increases in various antioxidant enzyme activities, including CAT, SOD, glutathione peroxidase, and GST in male mice. Furthermore, Ince et al. (2013) found that mice given oral doses of 15 mg/kg/day of Imidacloprid for 28 days exhibited a significant increase in malondialdehyde (MDA) levels, along with decreased SOD and CAT activities.

By isolating the mitochondria, we were able to illustrate a disturbance in both their structural integrity and energy-related functions, such as oxygen consumption, membrane permeability and swelling. Our findings reveal significant alterations in mitochondrial function (Table 4; Figs. 1, 2 and 3), indicative of neurotoxicity induced by IMI exposure.

Mitochondria, which are vital for energy production and cellular homeostasis, are particularly susceptible to Imidacloprid (IMI) exposure, resulting in significant disruptions to their structural and functional integrity. Our findings demonstrate that IMI exposure leads to impaired mitochondrial functions, including reduced oxygen consumption, increased swelling, and altered membrane permeability, which collectively contribute to mitochondrial dysfunction (Cestonaro et al. 2023). These observations suggest that mitochondria are primary targets of IMI-induced cytotoxicity.

A key concern is the observed increase in mitochondrial swelling, a precursor to cell death, as excessive or prolonged

swelling can cause the mitochondrial outer membrane to rupture, releasing pro-apoptotic proteins and initiating apoptosis. This mechanism links IMI exposure to potential neuronal apoptosis or cell death within the central nervous system (CNS) of mammals, paralleling findings in insect CNS studies (Sun et al. 2016; Chapa-Dubocq et al. 2017).

The underlying mechanism of mitochondrial swelling involves calcium overload, which promotes nitric oxide formation and activates enzymes that generate reactive oxygen species (ROS). This cascade disrupts ion homeostasis, releases pro-apoptotic factors, and amplifies oxidative stress, resulting in cellular damage (Sun et al. 2016). The resulting oxidative stress severely impairs mitochondrial structural integrity and function, as evidenced by decreased oxygen consumption rates, consistent with previous research as Gasmi et al. (2017).

Our study also found a highly significant increase ($p \leq 0.001$) in cerebral tissue swelling, suggesting potential inflammation and edema in the forebrain region (Figs. 1 and 3). This finding aligns with evidence that IMI exposure disrupts mitochondrial function in the CNS, potentially leading to apoptosis or programmed cell death (Table 4). These results underscore the neurotoxic potential of IMI and provide critical insights into how its exposure might contribute to neuronal damage (Lin and Beal 2006).

The stability of lysosomal membranes can be influenced by different environmental stressors in a dose-dependent manner, and an assay using neutral red can help identify the nature and degree of stress. Neutral red, a cationic probe and lipophilic compound employed as a dye, can penetrate cell membranes (Lowe et al. 1992).

In this work, Lysosomal destabilization was observed through the Neutral Red Retention Time assay, revealing significant changes in absorbance after 24 and 48 h in treated groups (Table 5; Fig. 4), aligning with findings by Sargent et al. 2021, who highlighted lysosomal dysfunction as a consequence of imidacloprid exposure. These results are consistent with previous studies by Martinez-Gomez et al. (2008) and Zhao et al. (2011), examined the effects of Pyrethroid on lysosomal membrane fragility by evaluating the retention time of the neutral red probe within the lysosomal compartment of both control and treated hemocytes.

Moreover, a qualitative assessment of lysosomal pH variations indicated a significant increase in pH in IMI-exposed groupsy (Figs. 10 and 11), emphasizing the impact of chronic pesticide exposure on lysosomal function. When the cell dies or the pH gradient is reduced, the dye cannot be retained (Filman et al 1975).

Microscopic observations are presented in Figs. 5, 6, 7 and 8 further demonstrated morphological alterations in lysosomal structures, suggesting potential membrane disruption. This is consistent with the results reported by Borenfreund and Puerner (1984), who demonstrated Maintaining a lower pH than that of the cytoplasm allows for dye retention within lysosomes, facilitating the differentiation between viable, damaged, or dead cells based on dye uptake and release dynamics.

The NRR assay on brain cells from *Wistar* rats exposed to 50 mg/kg of Imidacloprid revealed a notable "rounding-up" effect, where cells became more spherical, suggesting compromised cell membrane integrity (Fig. 5). This alteration likely facilitated the leakage of neutral red dye into the cytosol, indicating membrane disruption. Additionally, the presence of granulocytes with small lysosomes suggests that Imidacloprid exposure may also affect lysosomal structure and function in these cells.

The histopathological examination revealed marked neuronal degeneration, gliosis, and nuclear condensation (Fig. 9), confirming the cytotoxic impact of IMI on brain tissues. Our findings align with those of Bhardwaj et *al.*, who observed significant changes in brain sections of rats treated with 80 mg/kg body weight, including pronounced congestion in the cerebellum, degeneration of Purkinje cells with dendritic loss, vacuolation around neurons, and shrunken neurons by the 14th day of the experiment (Soujanya et al. 2013).

Overall, the study provides comprehensive insights into the multi-faceted neurotoxic impacts on the central nervous system induced by Imidacloprid, shedding light on the intricate interplay between oxidative stress, lysosomal integrity, and mitochondrial function in response to pesticide exposure.

Conclusion

This study highlights the harmful effects of Imidacloprid (IMI) on the brains of *Wistar* rats, revealing significant changes in redox markers, mitochondrial stress, and lysosomal stability. The findings indicate oxidative stress, mitochondrial dysfunction, and lysosomal destabilization, supported by histological alterations such as neuronal disorganization and evidence of neuroinflammation. The observed progression of lysosomal changes, from expansion to dye leakage and cell rounding, emphasizes the dynamic neurotoxic responses to IMI. Overall, these results underscore the complex interactions between oxidative stress and cellular integrity in the central nervous system, reinforcing the need for further research to understand the long-term impacts of neonicotinoid pesticides and their ecological implications.

Abbreviations IMI: Imidacloprid; CAT: Catalase; GPx: Glutathione Peroxidase; SOD: Superoxide Dismutase; GST: Glutathione S-Transferase; GSH: Glutathione; MDA: Malondialdehyde; MitCAT : Mitochondrial Catalase; MitGSH: Mitochondrial Glutathione; MitGPx: Mitochondrial Glutathione Peroxidase; MitGST: Mitochondrial

Glutathione S-Transferase; MitMDA: Mitochondrial Malondialdehyde; MitSOD: Mitochondrial Superoxide Dismutase; API: Algeria Pasteur Institute; FAO: Food and Agriculture Organization; EPA: Environmental Protection Agency; WHO: World Health Organization; H&E: Hematoxylin-Eosin (staining technique); HEPES: 4-(2-Hydroxyethyl)-1-piperazineethanesulfonic acid; IACUC: Institutional Animal Care and Use Committee; LD50: Lethal Dose, 50%; DMSO: Dimethyl Sulfoxide; CT: Control Group; ANOVA: Analysis of Variance; PBS: Phosphate-Buffered Saline; MPTP: Mitochondrial Permeability Transition Pore; NRRT: Neutral Red Retention Time; OD: Optical Density; ROS: Reactive Oxygen Species; SD: Standard Deviation; SE: Standard Error; NS: Not Significant; ΔOD/Δt: Change in Optical Density over Time

Authors contributions All authors contributed to the study conception and design. Material preparation, data collection and analysis were performed by Professor Rachid Rouabhi, and Sarra Zouaoui. The first draft of the manuscript was written by Rachid Rouabhi and Sarra Zouaoui, all authors commented on previous versions of the manuscript. All authors read and approved the final manuscript.

Funding None.

Data availability The data that support the findings of this study are not openly available due to reasons of sensitivity and are available from the corresponding author upon reasonable request.

Declarations

Ethical approval The authors declare that they respect the ethical handling and treatment of animals according the known ethical.

The submitted work is original work and not have been published elsewhere in any form or language (partially or in full).

Consent to participant Not applicable.

Consent to publish The participant has consented to the submission of the case report to the journal.

Competing interests The authors declare that they have no known competing financial interests or personal relationships that could have appeared to influence the work reported in this paper.

References

Aebi H (1984) Catalase in vivo. Methods Enzymol 105:121–126

Andjelkovic M, Buha-Djordjevic A, Antonijevic E et al (2019) Toxic effect of acute cadmium and lead exposure in rat blood, liver, and kidney. Int J Environ Res Public Health 16(2):274

Andra SS, Austin S, Kumar D et al (2017) Trends in the application of high-resolution mass spectrometry for human biomonitoring: an analytical primer to studying the environmental chemical space of the human exposome. Environ Int 100:32–61

Asghari MH, Moloudizargari M, Bahadar H, Abdollahi M (2017) A review of the protective effect of melatonin in pesticide-induced toxicity. Expert Opin Drug Metab Toxicol 13:545–554. https://doi.org/10.1080/17425255.2016.1214712

AsharWaheed MP, Muthu Mohammed HS (2012) Fenvalerate induced hepatotoxicity and its amelioration by quercetin. Int J Pharm Tech Res 4(4):1391–1400

Balani T, Agrawal S, Thaker AM (2011) Hematological and biochemical changes due to short-term oral administration of imidacloprid. Toxicol Int 18(1):2. https://doi.org/10.4103/0971-6580.75843

Beauchamp C, Fridovich I (1971) Superoxide dismutase: improved assays and an assay applicable to acrylamide gels. Biochem 44:276–287

Birsen A (2011) Effects of thiacloprid, deltamethrin and their combination on oxidative stress in lymphoid organs, polymorphonuclear leukocytes and plasma of rats. Pest Biochem Physiol 100(2):165–171. https://doi.org/10.1016/j.pestbp.2011.03.006

Bishop CA, Woundneh MB, Maisonneuve F et al (2020) Determination of neonicotinoids and butenolide residues in avian and insect pollinators and their ambient environment in Western Canada (2017, 2018). Sci Total Environ 737:139386

Bomann R (1989) NTN 33893. Study for Acute Oral Toxicity to Mice. Bayer AG. Fachbereich Toxikologie Wuppertal, Germany. Study No. 100039. DPR Vol. 51950–0003 # 119462

Borenfreund E, Puerner JA (1984) A simple quantitative procedure using monolayer cultures for cytotoxicity assays (HTD/NR90). J Tissue Cult Methods 9:7–9

Bradford M (1976) A rapid and sensitive method for the quantities of microgram quantities of protein utilizing the principle of protein-dye binding. Ann Biochem 11(72):248–254

Cesen MH, Pegan K, Spes A, Turk B (2012) Lysosomal pathways to cell death and their therapeutic applications. Exp Cell Res 318:1245–1251

Cestonaro LV, Crestani RP, Conte FM et al (2023) Immunomodulatory effect of imidacloprid on macrophage RAW 264.7 cells. Environ Toxicol Pharmacol 101:104190. https://doi.org/10.1016/j.etap.2023.104190

Chapa-Dubocq X, Makarov V, Javadov S (2017) Simple kinetic model of mitochondrial swelling in cardiac cells. J Cell Physiol. https://doi.org/10.1002/jcp.26335

Cimino AM, Boyles AL, Thayer KA, Perry MJ (2017) Effects of neonicotinoid pesticide exposure on human health: A systematic review. Environ Health Perspect 125:155–162

Clayton DA, Shadel GS (2014) Isolation of mitochondria from tissue culture cells. Cold Spring Harb Protoc. https://doi.org/10.1101/pdb.prot080002

Coremen M, Turkyilmaz IB,Us H, Us AS, Celik S, Ozel AE, Bulan OK, Yanardag R (2022) Lupeol inhibits pesticides induced hepatotoxicity via reducing oxidative stress and inflammatory markers in rats. Food Chem Toxicol 164:113068. https://doi.org/10.1016/j.fct.2022.113068

Cory-Slechta DA, Thiruchelvam M, Richfield EK et al (2005) Developmental pesticide exposures and the Parkinson's disease phenotype. Birth Defects Res A Clin Mol Teratol 73:136–139

Danyelle TM, Kenneth TD (2003) The role of glutathione-S-transferase in anticancer drug resistance. Oncogene 22:7369–7375

Dar AM, Khan MA, Raina R et al (2013) Effect of repeated oral administration of bifenthrin on lipid peroxidation and antioxidant parameters in Wistar rats. Bull Environ Contam Toxicol 91:125–128

Daubié S (2011) Neurobehavioral and physiological effects of low doses of polybrominated diphenyl ether (PBDE)-99 in male adult rats. Thesis of Doctorate, 201

De Duve C (1963) The lysosome concept. In: de Reuck AVS, Cameron MP (eds) Lysosomes. Churchill, London, pp 1–35

Douglas MR, Tooker JF (2015) Large-scale deployment of seed treatments has driven rapid increase in use of neonicotinoid insecticides and preemptive pest management in U.S. field crops. Environ Sci Technol 49:5088–5097

Duzguner V, Erdogan S (2010) Acute oxidant and inflammatory effects of imidacloprid on the mammalian central nervous system and liver in rats. Pest Biochem Physiol 97:13–18

EL-Gendy AK, Aly NM, Mahmoud FH, Kenawy A, El-Sebae AK (2010) The role of Vit C as antioxidant in protection of oxidative stress induced by imidacloprid. Food Chem Toxicol 48:215–221

Fang W, Peng Y, Muir D, Lin J, Zhang X (2019) A critical review of synthetic chemicals in surface waters of the US, the EU, and China. Environ Int 131:104994

Filman DJ, Brawn RJ, Dankler WB (1975) Intracellular supravital stain delocalization as an assay for antibody-dependent complement-mediated cell damage. J Immunol Methods 6:189–207

Fivenson EM, Lautrup S, Sun N, Scheibye-Knudsen M et al (2017) Mitophagy in neurodegeneration and aging. Neurochem Int 109:202–209

Flohe G (1984) Analysis of glutathione peroxidase. Methods Enzymol 105:114–121

Food and Agriculture Organization (FAO) (2020) Acceptable daily intakes, acute reference doses, residue definitions, recommended maximum residue limits, supervised trials median residue values and other values recorded. Joint FAO/WHO Meeting on Pesticide Residues

Fraldi A, Klein AD, Medina DL, Settembre C (2016) Brain disorders due to lysosomal dysfunction. Annu Rev Neurosci 39:277–295

Fujiwara Y, Kikkawa M, Okamura Y et al (2009) A new pH-sensitive fluorescent probe for lysosomes and its application to autophagy. FEBS J 276(18):5499–5512. https://doi.org/10.1111/j.1742-4658.2009.07289.x

Gasmi S, Kebieche M, Rouabhi R, Touahria C et al (2017) Alteration of membrane integrity and respiratory function of brain mitochondria in rats chronically exposed to a low dose of acetamiprid. Environ Sci Pollut Res 24:22258–22264

Habig WH, Pabst MJ, Jakoby WB (1974) Glutathione S-transferases: the first enzymatic step in mercapturic acid formation. J Biol Chem 249:7130–7139

Henine S, Rouabhi R, Gasmi S, Amrouche A et al (2016) Oxidative stress status, caspase-3, stromal enzymes, and mitochondrial respiration and swelling of Paramecium caudatum in response to Fe3O4 nanoparticles. Environ Health Sci 8:161

Houlot R (1984) Techniques d'histologie et de cytopathologie. Ed Maloine, pp 225–227

Ince S, Kucukkurt I, Demirel HH et al (2013) The role of thymoquinone as antioxidant protection on oxidative stress induced by imidacloprid in male and female Swiss albino mice. Toxicol Environ Chem 95:318–329

Jeschke P, Nauen R, Schindler M, Elbert A (2011) Overview of the status and global strategy for neonicotinoids. J Agric Food Chem 59:2897–2908

Julvez J, Mendez M, Fernandez-Barres S, Romaguera D et al (2016) Maternal consumption of seafood in pregnancy and child neuropsychological development: a longitudinal study. Am J Epidemiol 183(3):169–182

Kapoor U, Srivastava MK, Bhardwaj S, Srivastava LP (2010) Effect of imidacloprid on antioxidant enzymes and lipid peroxidation in female rats to derive its No Observed Effect Level (NOEL). J Toxicol Sci 35:577–581

Kara M, Yumrutas O, Demir CF, Ozdemir HH, Bozgeyik I, Coskun S, Eraslan E, Bal R (2015) Insecticide imidacloprid influences cognitive functions and alters learning performance and related gene expression in a rat model. Int J Exp Pathol 96:332–337. https://doi.org/10.1111/iep.12139

Karahan A, Çakmak I, Hranitz JM et al (2015) Sublethal imidacloprid effects on honeybee flower choices when foraging. Ecotoxicol 24(9):2017–2025

Li J, Yu W, Li X, Li B (2014) The effects of propofol on mitochondrial dysfunction following focal cerebral ischemia–reperfusion in rats. Neuropharmacol 77:358–368

Lin MT, Beal MF (2006) Mitochondrial dysfunction and oxidative stress in neurodegenerative diseases. Nat 7113:787–795

Lonare M, Kumar M, Raut S et al (2014) Evaluation of imidacloprid-induced neurotoxicity in male rats: A protective effect of curcumin. Neurochem Int 78:122–129

Lowe DM, Moore MN, Evans BM (1992) Contaminant impact on interactions of molecular probes with lysosomes in living hepatocytes from dab Limanda limanda. Mar Ecol Prog Ser 91:135–140

Lowe DM, Fossato VU, Delpedge MH (1995) Contaminant-induced lysosomal membrane damage in blood cells of mussels Mytilus galloprovincialis from Venice Lagoon: an in vitro study. Mar Ecol Prog Ser 129:189–196

Mani MV, Asha S, Sadiq MMA (2014) Pyrethroid deltamethrin-induced developmental neurodegenerative cerebral injury and ameliorating effect of dietary glycoside naringin in male Wistar rats. Biomed Aging Pathol 4:1–8

Martinez-Gomez C, Benedicto J et al (2008) Application and evaluation of the neutral red retention (NRR) assay for lysosomal stability in mussel populations along the Iberian Mediterranean coast. J Environ Monit 10:490–499

Mehta SK, Gowder SJT (2015) Members of antioxidant machinery and their functions. In: Gowder S.J.T. (Ed.), Basic Principles and Clinical Significance of Oxidative Stress. IntechOpen 61–85. https://doi.org/10.5772/59293

Miao Z, Wang S, Wu H, Xu S (2022) Exposure to imidacloprid induces oxidative stress, mitochondrial dysfunction, inflammation, apoptosis, and mitophagy via NF-kappaB/JNK pathway in grass carp hepatocytes. Fish Shellfish Immunol 120:674–685. https://doi.org/10.1016/j.fsi.2021.12.017

Mikolić A, Karačonji IB (2018) Imidacloprid as reproductive toxicant and endocrine disruptor: Investigations in laboratory animals. Arch Ind Hyg Toxicol 69(2):103–108. https://doi.org/10.2478/aiht-2018-69-3144

Mohany M, Badr G, Refaat I, El-Feki M (2011) Immunological and histological effects of exposure to imidacloprid insecticide in male albino rats. African J Pharm Pharmacol 5(18). https://doi.org/10.5897/AJPP11.625

Pauluhn J (1988) Study for acute inhalation toxicity in the rat. Bayer AG, Fachbereich Toxikologie, Wuppertal, Germany. Study No. 99806. DPR Vol. 51950–0002 119449

PNEU/RAMOGE (1999) Manuel sur les biomarqueurs recommandés pour le programme de Biosurveillance du MED POL. Programme des Nations Unies pour l'Environnement

Pryde KR, Hirst J (2011) Superoxide is produced by the reduced flavin in mitochondrial complex I: A single, unified mechanism that applies during both forward and reverse electron transfer. J Biol Chem 286:18056–18065

Repetto G, Sanz P (1993) Neutral red uptake, cellular growth, and lysosomal function: In vitro effects of 24 metals. Altern Lab Anim 21:501–507

Rouabhi R, Gasmi S, Boussekine S, Kebieche M (2015) Hepatic oxidative stress induced by Zn and opposite effect of Se in Oryctolagus cuniculus. J Environ Anal Toxicol 289:10–4172

Sakthiselvi T, Paramasivam M, Vasanthi D, Bhuvaneswari K (2020) Persistence, dietary, and ecological risk assessment of indoxacarb residue in/on tomato and soil using GC-MS. Food Chem 328:127134

Sargent D, Cunningham LA, Dues DJ, Yue M, Kordich JJ, Mercado G, Brundin P, Cowell RM, Moore DJ (2021) Neuronal *VPS35* deletion induces spinal cord motor neuron degeneration and early post-natal lethality. Brain Commun 3(3):1–20. https://doi.org/10.1093/braincomms/fcab208

Sheets LP (2001) A Developmental neurotoxicity study with technical grade imidacloprid in wistar rats. Bayer Corporation, Agricultural Division Toxicology, Kansas, USA. Study No. 110245. DPR Vol. 51950–0474 # 209393

Simon-Delso N, Amaral-Rogers V, Belzunces LP et al (2015) Systemic insecticides (neonicotinoids and fipronil): Trends, uses, mode of action, and metabolites. Environ Sci Pollut Res 22:5–34

Soujanya S, Lakshman M, Kumar AA, Reddy AG (2013) Evaluation of the protective role of vitamin C in imidacloprid-induced hepatotoxicity in male albino rats. J Natural Sci Biol Med 4:637

Sun Q, Xiao X, Kim Y et al (2016) Imidacloprid promotes high-fat diet-induced adiposity and insulin resistance in male C57BL/6J mice. J Agric Food Chem. https://doi.org/10.1021/acs.jafc.6b04322

Tomlin CDS (2006) The Pesticide Manual: A World Compendium (14th ed.). British Crop Protection Council, Alton, Hampshire, 186–187

U.S. Environmental Protection Agency (EPA) (2021) Pesticide limits. https://www.epa.gov/pesticides

Utami RR, Geerling GW et al (2020) Environmental prioritization of pesticides in the Upper Citarum River Basin, Indonesia, using predicted and measured concentrations. Sci Total Environ 738:140130

Valdovinos-Flores C, Gosenbatt ME (2012) The role of amino acids transporters in GSH synthesis in the blood-brain barrier and central nervous system. Neurochem Int 61:405–414

Wang Y, Balaji V, Kaniyappan S et al (2017) The release and transsynaptic transmission of Tau via exosomes. Mol Neurodegener 12:5

Wang X, Anadón A, Wu Q et al (2018) Mechanism of neonicotinoid toxicity: Impact on oxidative stress and metabolism. Annual Rev Pharmacol Toxicol 58:471–507

Warso MA, Lands WE (1983) Lipid peroxidation in relation to prostacyclin and thromboxane physiology and pathophysiology. British Med Bull 39:277–280

Weckbercker G, Cory JG (1988) Ribonucleotide reductase activity and growth of glutathione-dependent mouse leukemia L1210 cells in vitro. Cancer Lett 40(3):257–264

WHO/FAO (2019) Acceptable daily intakes, acute reference doses, acute and long-term dietary exposures, recommended maximum residue levels, supervised trials median residue values and other values recorded by the 2019 extra meeting. Joint FAO/WHO meeting on pesticide residues. Summary report, 11 p

Xu X, Wang X, Yang Y et al (2022) Neonicotinoids: Mechanisms of systemic toxicity based on oxidative stress-mitochondrial damage. Arch Toxicol 96:1493–1520. https://doi.org/10.1007/s00204-022-03267-5

Zhang Y-T, Zheng Q-S, Pan J, Zheng R-L (2004) Oxidative damage of biomolecules in mouse liver induced by morphine and protected by antioxidants. Basic Clin Pharmacol Toxicol 95(2):53–58. https://doi.org/10.1111/j.1742-7843.2004.950202.x

Zhao C, Li X, Luo S, Chang Y (2011) Assessments of lysosomal membrane responses to stresses with neutral red retention assay and its potential application in the improvement of bivalve aquaculture. Afr J Biotech 10(64):13968–13973

Zhao G-P, Yang F-W et al (2020) Toxicities of neonicotinoid-containing pesticide mixtures on nontarget organisms. Environ Toxicol Chem. https://doi.org/10.1002/etc.4842

Authors and Affiliations

Sarra Zouaoui[1,2] · Rachid Rouabhi[1,2]

✉ Rachid Rouabhi
r_rouabhi@univ-tebessa.dz

[1] Laboratory of Toxicology and Ecosystems Pathologies, Echahid Cheikh Larbi Tebessi University, Tebessa, Algeria

[2] Applied Biology Department, Echahid Cheikh Larbi Tebessi University, Tebessa, Algeria

Terms and Conditions

Springer Nature journal content, brought to you courtesy of Springer Nature Customer Service Center GmbH (“Springer Nature”).
Springer Nature supports a reasonable amount of sharing of research papers by authors, subscribers and authorised users (“Users”), for small-scale personal, non-commercial use provided that all copyright, trade and service marks and other proprietary notices are maintained. By accessing, sharing, receiving or otherwise using the Springer Nature journal content you agree to these terms of use (“Terms”). For these purposes, Springer Nature considers academic use (by researchers and students) to be non-commercial.
These Terms are supplementary and will apply in addition to any applicable website terms and conditions, a relevant site licence or a personal subscription. These Terms will prevail over any conflict or ambiguity with regards to the relevant terms, a site licence or a personal subscription (to the extent of the conflict or ambiguity only). For Creative Commons-licensed articles, the terms of the Creative Commons license used will apply.
We collect and use personal data to provide access to the Springer Nature journal content. We may also use these personal data internally within ResearchGate and Springer Nature and as agreed share it, in an anonymised way, for purposes of tracking, analysis and reporting. We will not otherwise disclose your personal data outside the ResearchGate or the Springer Nature group of companies unless we have your permission as detailed in the Privacy Policy.
While Users may use the Springer Nature journal content for small scale, personal non-commercial use, it is important to note that Users may not:

1. use such content for the purpose of providing other users with access on a regular or large scale basis or as a means to circumvent access control;
2. use such content where to do so would be considered a criminal or statutory offence in any jurisdiction, or gives rise to civil liability, or is otherwise unlawful;
3. falsely or misleadingly imply or suggest endorsement, approval , sponsorship, or association unless explicitly agreed to by Springer Nature in writing;
4. use bots or other automated methods to access the content or redirect messages
5. override any security feature or exclusionary protocol; or
6. share the content in order to create substitute for Springer Nature products or services or a systematic database of Springer Nature journal content.

In line with the restriction against commercial use, Springer Nature does not permit the creation of a product or service that creates revenue, royalties, rent or income from our content or its inclusion as part of a paid for service or for other commercial gain. Springer Nature journal content cannot be used for inter-library loans and librarians may not upload Springer Nature journal content on a large scale into their, or any other, institutional repository.
These terms of use are reviewed regularly and may be amended at any time. Springer Nature is not obligated to publish any information or content on this website and may remove it or features or functionality at our sole discretion, at any time with or without notice. Springer Nature may revoke this licence to you at any time and remove access to any copies of the Springer Nature journal content which have been saved.
To the fullest extent permitted by law, Springer Nature makes no warranties, representations or guarantees to Users, either express or implied with respect to the Springer nature journal content and all parties disclaim and waive any implied warranties or warranties imposed by law, including merchantability or fitness for any particular purpose.
Please note that these rights do not automatically extend to content, data or other material published by Springer Nature that may be licensed from third parties.
If you would like to use or distribute our Springer Nature journal content to a wider audience or on a regular basis or in any other manner not expressly permitted by these Terms, please contact Springer Nature at

onlineservice@springernature.com